

10/30/96 JSD

LBL-37983 Rev. 1
UC-413

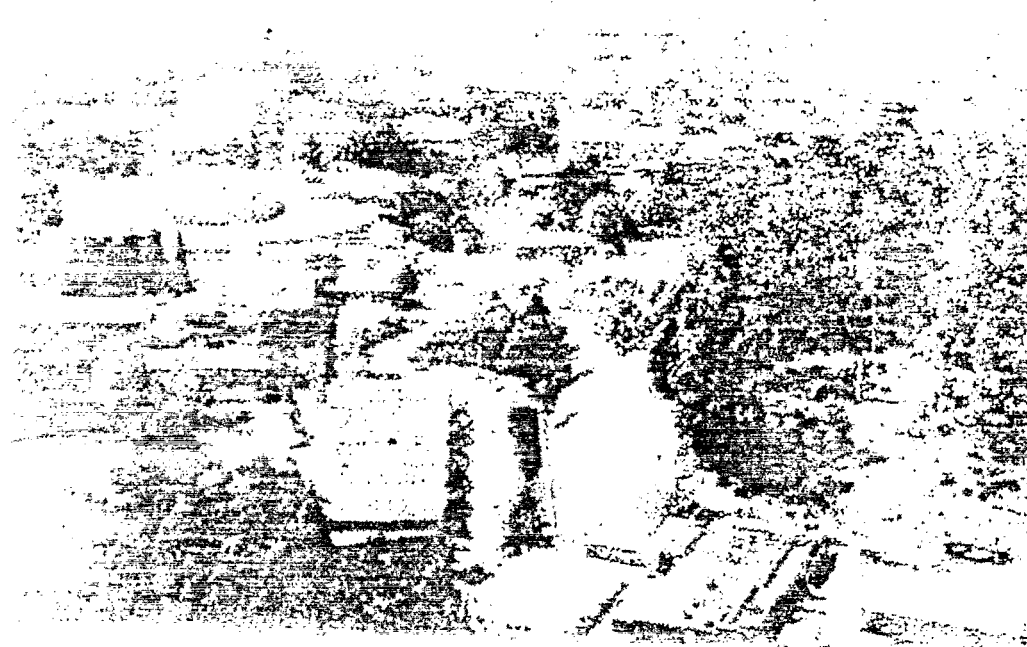


ERNEST ORLANDO LAWRENCE BERKELEY NATIONAL LABORATORY

Optimization of the $^7\text{Li}(\text{p},\text{n})$ Proton Beam Energy for BNCT Applications

**D.L. Bleuel and R.J. Donahue
Environment, Health
and Safety Division**

May 1996



DISTRIBUTION OF THIS DOCUMENT IS UNLIMITED

kg **MASTER**

DISCLAIMER

This document was prepared as an account of work sponsored by the United States Government. While this document is believed to contain correct information, neither the United States Government nor any agency thereof, nor The Regents of the University of California, nor any of their employees, makes any warranty, express or implied, or assumes any legal responsibility for the accuracy, completeness, or usefulness of any information, apparatus, product, or process disclosed, or represents that its use would not infringe privately owned rights. Reference herein to any specific commercial product, process, or service by its trade name, trademark, manufacturer, or otherwise, does not necessarily constitute or imply its endorsement, recommendation, or favoring by the United States Government or any agency thereof, or The Regents of the University of California. The views and opinions of authors expressed herein do not necessarily state or reflect those of the United States Government or any agency thereof, or The Regents of the University of California.

Available to DOE and DOE Contractors
from the Office of Scientific and Technical Information
P.O. Box 62, Oak Ridge, TN 37831
Prices available from (615) 576-8401

Available to the public from the
National Technical Information Service
U.S. Department of Commerce
5285 Port Royal Road, Springfield, VA 22161

Ernest Orlando Lawrence Berkeley National Laboratory
is an equal opportunity employer.

Optimization of the $^7\text{Li}(\text{p},\text{n})$ Proton Beam Energy for BNCT Applications

B.L. Bleuel^a and R.J. Donahue^b

^aNuclear Engineering Department, University of California, Berkeley, CA 94720

^bEnvironment, Health and Safety Division, Ernest Orlando Lawrence Berkeley National Laboratory, University of California, Berkeley, CA 94720

May 1996

This work was supported by the Director, Office of Energy Research, Nuclear Physics Division of the Office of High Energy and Nuclear Physics, of the U.S. Department of Energy under Contract No. DE-AC03-76SF00098.

DISCLAIMER

**Portions of this document may be illegible
in electronic image products. Images are
produced from the best available original
document.**

Optimization of the $^7\text{Li}(\text{p},\text{n})$ Proton Beam Energy for BNCT Applications

D. L. Bleuel^a and R. J. Donahue^b

^a Nuclear Engineering Department, University of California, Berkeley, CA 94720

^b Lawrence Berkeley National Laboratory, Berkeley, CA 94720

ABSTRACT

The reaction $^7\text{Li}(\text{p},\text{n})^7\text{Be}$ has been proposed as an accelerator-based source of neutrons for Boron Neutron Capture Therapy (BNCT). This reaction has a large steep resonance for proton energies of about 2.3 MeV which ends at about 2.5 MeV. It has generally been accepted that one should use 2.5 MeV protons to get the highest yield of neutrons for BNCT. This paper suggests that for BNCT the optimum proton energy may be about 2.3 MeV and that a proton energy of about 2.2 MeV will provide the same useful neutron flux outside a thinner moderator as the neutron flux from a 2.5 MeV proton beam with a thicker moderator. These results are based on optimization of the useful neutron spectrum in air at the point of irradiation, not on depth-dose profiles in tissue/tumor.

This work was supported by the Director, Office of Energy Research, Nuclear Physics Division of the Office of High Energy and Nuclear Physics, of the U. S. Department of Energy under Contract DE-AC03-76SF00098

Introduction

Boron Neutron Capture Therapy (BNCT) is a treatment modality for cancer that depends on an uptake of boron by tumor cells and then the exposure of these boron-loaded tumor cells to thermal neutrons. This treatment is particularly promising for deep-seated brain tumors which are inoperable. The reaction $^{10}\text{B}(\text{n},\alpha)^7\text{Li}$ produces high LET products whose ranges are roughly equivalent to the diameter of cancer cells ($\tilde{10} \mu\text{m}$). Interest in BNCT has been renewed due to research into a new generation of boronated drugs which show a selectively high uptake in animal tumors. For example a recent study by Hill¹ has measured selective tumor uptakes of boronated protoporphyrin (BOPP) as high as 400:1 relative to normal brain blood concentrations in mice.

Blue and colleagues²⁻⁴ have published a great deal of work on accelerator-based BNCT facilities. The majority of accelerator-based BNCT proposals to date involve 2.5 MeV protons incident on a metal ^7Li target, utilizing the $^7\text{Li}(\text{p},\text{n})^7\text{Be}$ reaction to produce neutrons. These neutrons must be slowed down in energy, via a filter (moderator/reflector) assembly, by roughly 2-4 orders of magnitude for BNCT treatments since the neutron distribution from the target peaks in the energy range of 400 to 700 keV in the forward direction for 2.5 MeV incident protons. The generally accepted³ useful neutron energy range from the filter assembly for treating deep-seated tumors is 1 eV to 10 keV. In this paper we examine the optimum proton beam energy for different moderator and reflector combinations to produce the best neutron characteristics for BNCT.

Neutron Source Characterization

The reaction $^7\text{Li}(\text{p},\text{n})^7\text{Be}$ displays a large resonance in the forward direction around 2.3 MeV which extends to about 2.5 MeV. It has been generally accepted that to get the highest neutron yield for BNCT one should use a proton beam energy of 2.5 MeV. However this is a careful tradeoff between neutron yield and neutron spectrum from the target. Upon close examination of the $^7\text{Li}(\text{p},\text{n})$ cross sections⁵ it appeared that a proportionally large high-energy tail is produced as one increases the incident proton energy. It was decided that these tradeoffs were not completely apparent and that a careful examination was needed.

A fortran program[†] was written to calculate neutron double differential (angle and energy) distributions from the target as a function of incident proton beam energy. Liskien⁵ has derived center of mass best values for normalized Legendre coefficients for predicting cross sections for the $^7\text{Li}(\text{p},\text{n})^7\text{Be}$ reaction. For a given proton energy the cross section, as a function of center of mass angle, can be determined in the center of mass system by:

$$\frac{d\sigma}{d\omega}(\phi) = \frac{d\sigma}{d\omega}(0^\circ) \sum_i A_i P_i(\phi) \quad (1)$$

where A_i are the coefficients of the Legendre polynomials determined by Liskien and $P_i(\phi)$ are the Legendre polynomials as a function of center of mass scattered angle. The total cross section integrated over all angles is simply given by:

$$\sigma = 4\pi \left(\frac{d\sigma}{d\omega}(0^\circ) \right) A_0 \quad (2)$$

The Legendre coefficients are normalized such that

$$\sum_i A_i = 1.0 \quad (3)$$

Transformation from center of mass system variables to laboratory system is determined by the following relation⁶

[†] The program lipn.f is available via anonymous ftp at fubar.lbl.gov (IP 131.243.214.19).

$$\cos\theta = \frac{\cos\phi + \rho}{\sqrt{1 + 2\rho\cos\phi + \rho^2}} \quad (4)$$

where ρ is defined as

$$\rho = \frac{m_p}{m_n \sqrt{1 + \frac{m_p + m_n}{m_n} \frac{Q}{E}}} \quad (5)$$

The relation between the center of mass cross section and the laboratory system cross section is given by⁶

$$\sigma(\theta) = \sigma(\phi) \frac{(1 + 2\rho\cos\phi + \rho^2)^{\frac{3}{2}}}{1 + \rho\cos\phi} \quad (6)$$

The neutron energy is determined by the following relation⁷

$$E_n = E_p \frac{m_p m_n}{(m_n + m_r)^2} \left\{ 2\cos^2\theta + \frac{m_r(m_r + m_n)}{m_p m_n} \left[\frac{Q}{E_p} + \left(\frac{1 - m_p}{m_r} \right) \right] \right. \\ \left. \pm 2\cos\theta \sqrt{\cos^2\theta + \frac{m_r(m_r + m_n)}{m_p m_n} \left[\frac{Q}{E_p} + \left(\frac{1 - m_p}{m_r} \right) \right]} \right\} \quad (7)$$

where E_n and E_p are the neutron and proton kinetic energies, m_n and m_p their respective masses, m_r the target residual mass (*i.e.*⁷Be). The Q value for this reaction is given as⁵ 1.644 MeV. The reaction thresholds are given by Liskien as 1.881 MeV in the forward direction and 1.920 MeV in the backward direction. In our program the threshold, which is used to determine the target thickness, is assumed to be 1.950 MeV as this is as low as Liskien's Legendre coefficients were fitted to experimental data.

Only the reaction ⁷Li(p,n)⁷Be is considered. The reaction ⁷Li(p,n)⁷Be* which produces a 0.431 MeV gamma with a threshold of 2.373 MeV in the forward direction and 2.423 MeV in the backward direction, and the reaction ⁷Li(p,n)⁷Be** which produces a 4.55 MeV gamma with a threshold of 7.08 MeV are not considered in our treatment. These cross sections are generally only a few percent of the

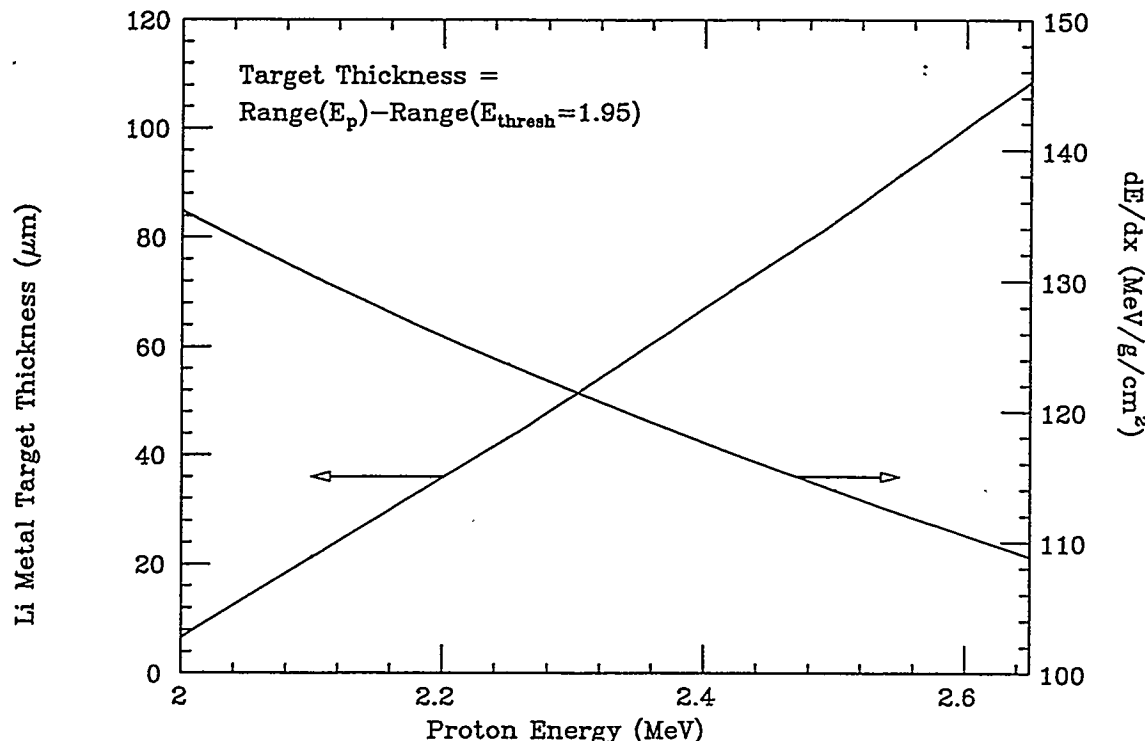


Figure 1: ${}^7\text{Li}$ metal target thickness as a function of incident proton kinetic energy.

${}^7\text{Li}(\text{p},\text{n}){}^7\text{Be}$ cross section at proton energies less than or equal to 2.5 MeV. In addition the breakup reaction ${}^7\text{Li}(\text{p},\text{n}{}^3\text{He}){}^4\text{He}$ with a threshold at 3.692 MeV is not considered.

The target thickness is calculated by subtracting the range of the incident proton from the range of a proton at the threshold energy in Li metal. In this way only protons with energies at or above the reaction threshold are allowed to deposit any energy directly in the target to minimize heating of the target. Range and stopping power data are taken from Janini⁸ with log-log interpolation for intermediate energy values. Target thickness calculated by this program for various incident proton kinetic energies is shown in Fig. 1.

The target is then subdivided into 100 equal thickness subregions. In each region the sampled stopping power is used to determine the current proton beam energy, the Legendre coefficients are sampled and then the cross sections are determined

according to Eqs. (1) and (6) over 1° angle increments. For each subregion a check is made to ensure that

$$\sigma = \int_0^{2\pi} \int_0^\pi \frac{d\sigma}{d\omega_L} = \int_0^{2\pi} \int_0^\pi \frac{d\sigma}{d\omega_C} = 4\pi \left(\frac{d\sigma}{d\omega} \right) (0^\circ) A_0 \quad (8)$$

where $d\omega_L$ and $d\omega_C$ are the lab system and center of mass system differential solid angles.

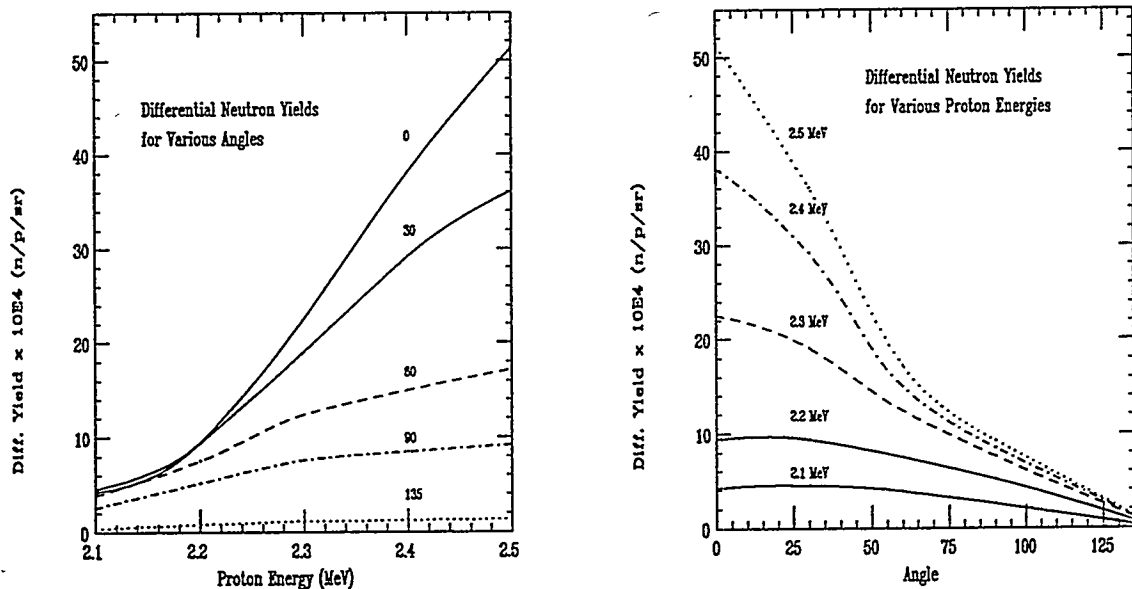


Figure 2: Differential neutron yields for protons on ${}^7\text{Li}$ metal target.

For each proton energy and each sampled angle the neutron energy is calculated from Eq. (7). From this the overall double differential neutron production probabilities can be estimated for each incident proton beam energy from the accelerator. These are shown in Fig. 2.

The neutron energy spectra for various angle bins and for various incident proton kinetic energies are shown in Fig. 3. This information is used as the starting point for subsequent simulations of neutron transport in various moderator and reflector materials. Total neutron yields, integrated over all neutron energies and angles, are shown in Table 1.

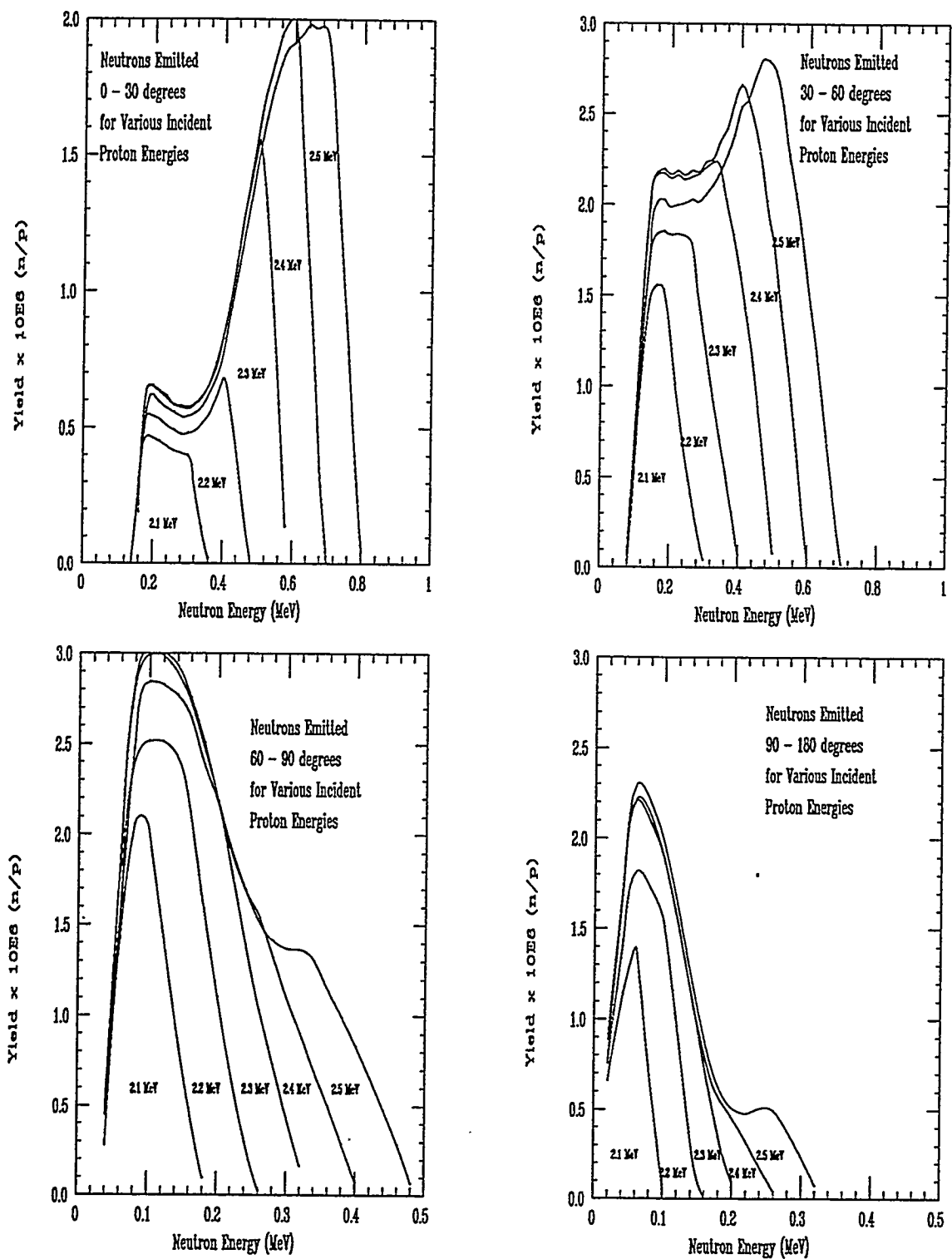


Figure 3: Neutron yields (per incident proton) as a function of neutron energy for different angle bins and various incident proton kinetic energies for the ${}^7\text{Li}(p,n){}^7\text{Be}$ reaction.

Table 1: Total neutron yield as a function of incident proton energy (neutrons/incident proton).

E_p (MeV)	Yield (n/p)
2.1	2.69×10^{-5}
2.2	5.45×10^{-5}
2.3	9.26×10^{-5}
2.4	1.23×10^{-4}
2.5	1.46×10^{-4}
2.6	1.68×10^{-4}

Moderator Design and Modeling

To be useful in BNCT applications, the neutron spectra portrayed in Fig. 3 must be moderated sufficiently such that a maximum flux of useful epithermal neutrons is delivered to the patient while the dose due to non-useful neutrons is minimized. Several designs for beam shaping assemblies have been proposed for use in optimizing neutron beam characteristics for BNCT. These designs are normally optimized to deliver the best neutron spectra for a given 2.5 MeV proton incident beam. Such designs must be modified for lower energy proton beams, as the lower neutron energies produced in the $^7\text{Li}(p,n)\text{Be}$ reaction need less moderation. Other factors, such as the reflector and beam delimiter configuration, normally do not need to be altered as their effect is largely independent of neutron energy.

The effect of changing the proton beam energy was analyzed on four different moderator designs, three of which have been proposed by Blue^{3,4} and one by Karni⁹. The basic assembly designs, which consist of a moderator, reflector, and beam delimiter, are shown in Fig. 4. The difference in these designs is primarily in the choice of moderator. These choices are listed in Table 1, along with the optimum moderator thickness for 2.5 MeV protons, as determined by the designer. The BeO design³ was originally determined to provide the best moderation for BNCT effective neutrons. It was discarded for practicality and materials issues for a design based on heavy water, which could produce similar, though less optimal, results. The $^7\text{LiF}/\text{Pb}$ design⁹ was optimized by a one-dimensional transport code

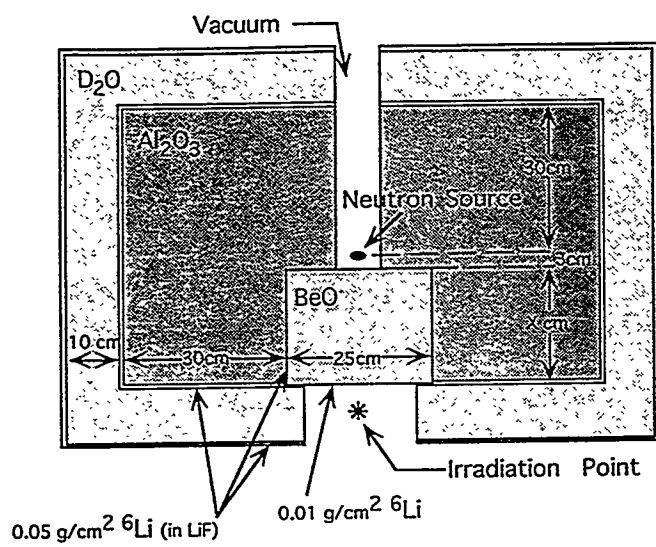
Table 2: Various moderator/reflector designs considered for optimization in this work.

#	Designed by	Moderator	Configuration optimized for 2.5 MeV p's
1	Blue ³	BeO	20.0 cm BeO, Al ₂ O ₃ reflector
2	Blue ³	D ₂ O	25.0 cm D ₂ O, Al ₂ O ₃ reflector
3	Karni ⁹	⁷ LiF/Pb	30.0 cm ⁷ LiF, 1.0 cm Pb, Al ₂ O ₃ refl.
4	Blue ⁴	D ₂ O	25.0 cm D ₂ O, Li ₂ CO ₃ reflector 30.0 cm diameter moderator 26.0 cm diameter accelerator beam port

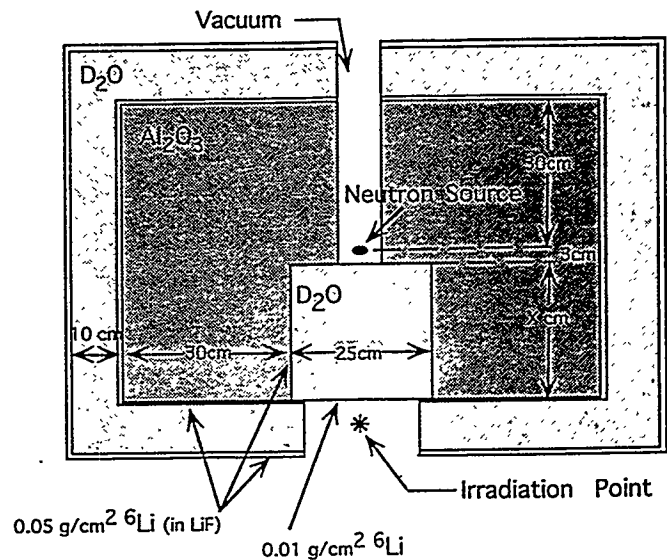
and did not originally include a reflector or beam delimiter, which were added in this analysis in order to effectively compare it to the other designs. The final design by Blue⁴ effects some modifications due to recent work, such as a Li₂CO₃ reflector, which produces fewer capture gamma rays than Al₂O₃, and a wider beam port and moderator to accomodate target heating problems. There are small structural differences between this model and Blue's final design. The general reflector and beam delimiter geometry were not changed from the first three models in Table 2, so as to make more accurate comparisons between this and the other designs, based only on the change in materials and moderator geometry.

These four assemblies were modeled using MCNP4¹⁰, a three dimensional, point-wise continuous cross-section Monte Carlo neutron/photon transport code to determine the optimum moderator thickness for each incident proton energy. ENDF/B-V cross section data is used. MCNP's use of "point-wise continuous cross-sections" means that linear interpolation between cross section data points over the entire energy range will reproduce the experimental cross section data to within 1%. The entire neutron source distribution mentioned earlier was modeled in 10° angle increments from 0° to 180° (azimuthally symmetric), with a distribution of 50 energy bins in each angle bin. In modeling the assembly, the thickness of the moderator was allowed to vary and for each thickness, the neutron flux spectrum in air at the patient window was determined.

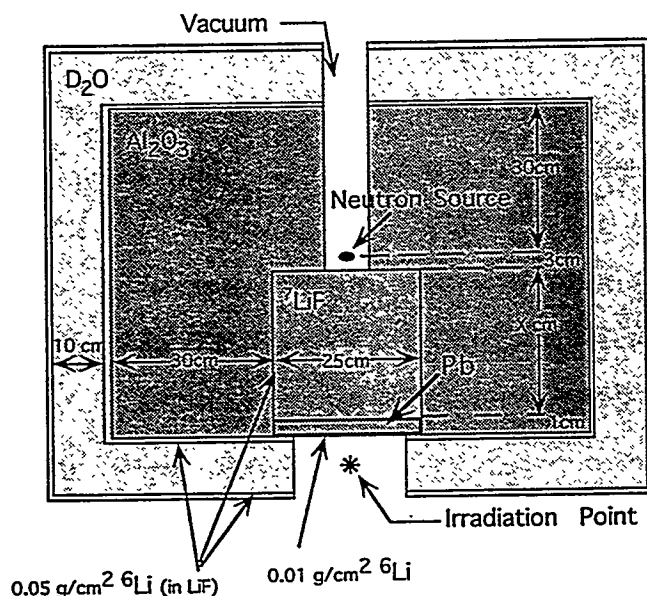
It is difficult to judge the effectiveness of a particular neutron spectrum in air for use in BNCT applications. The assembly designs that were developed by



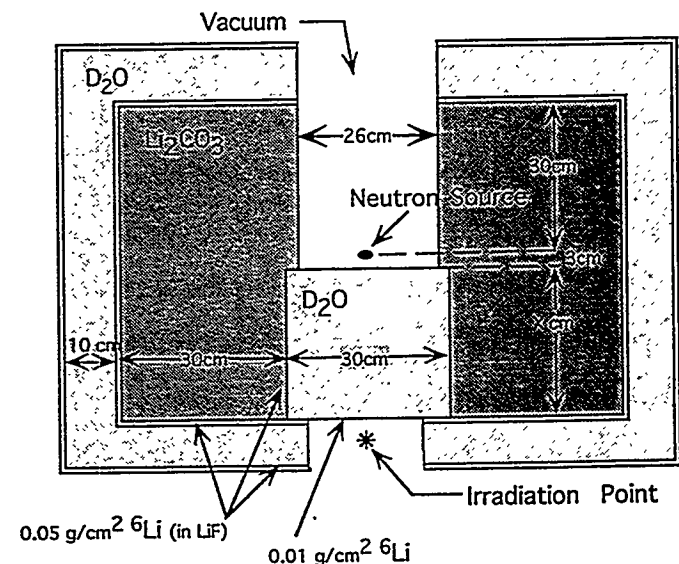
Assembly Design #1 (Blue et. al.)



Assembly Design #2 (Blue et. al.)



Assembly Design #3 (Greenspan)



Assembly Design #4 (Blue et. al.)

Figure 4: Configurations of four design assemblies considered here. These are cross-sections of cylindrical assemblies. Proton beam enters from the top of the assembly. Each design consists of a moderator, reflector and a $D_2O/{}^6\text{Li}$ neutron shield around the reflector. The moderator thickness ("x") is allowed to vary.

Blue and evaluated here were optimized by Blue using a parameter known as the RUFTED (Ratio of Useful Flux to Equivalent Dose), a parameter that we also use to determine the quality of a neutron flux. The RUFTED is defined as:

$$RUFTED = \frac{\Phi_u}{K_n \cdot RBE_n + K_\gamma}$$

Here, Φ_u is the useful neutron flux in $n/cm^2\text{-source neutron}$, K_γ is the gamma kerma in $cGy/source neutron$, K_n is the neutron kerma in $cGy/source neutron$, and $RBE_n(E)$ is the kerma-averaged neutron RBE (Relative Biological Effectiveness). The definition of the range of neutrons useful for BNCT is a matter of some debate and depends on many factors including tumor depth and Boron loading in the tumor and in normal tissue. It is generally accepted that 1 eV is an appropriate lower limit, with some considerable debate on the upper limit^{11,3}. For our calculations, Φ_u has been defined as the flux of neutrons at the irradiation point in the range of 1 eV-10 keV. Some testing has assured that the relative results in this paper are largely invariant to the exact definition of this range.

Of even greater debate than Φ_u is the debate over the definition of the neutron RBE. The energy dependent values given by Blue¹² were used here (see Fig. 5), as other choices only included distributions in inappropriate ranges¹³ for our purposes, or energy independent, constant values, which varied from 2 to 4. The questionable nature of the neutron RBE leads to uncertainty of its effect on our results and therefore we also analyzed the effect of using a constant neutron RBE of 2 and 3. Again, the relative results did not significantly differ and our conclusions were unchanged.

Φ_u is also an important parameter in optimizing a particular assembly design. Φ_u , however, is a measure of the useful neutron flux per source neutron. This should be normalized to the neutron yield per proton current, as lower energy protons at a given current will not yield as many source neutrons per second in the $^7\text{Li}(p,n)\text{Be}$ reaction, as shown in Table 2. Additionally, because a larger proton flux can be generated at lower energies, this parameter should also be normalized

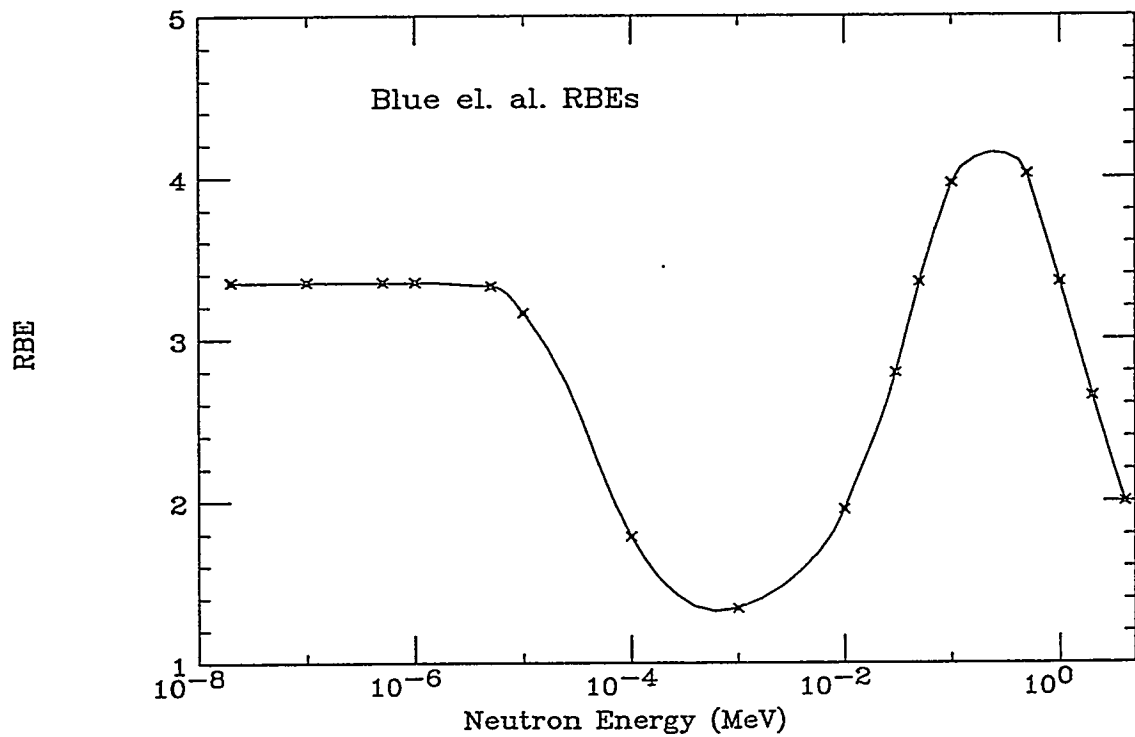


Figure 5: Neutron energy dependent RBE from Blue.

to the energy of the protons, making the optimization parameter $\Phi_{u/P}$ the useful flux per accelerator power in units of $\text{n/cm}^2\text{-s-kW}$:

$$\Phi_{u/P} = \Phi_u / (E_p \times Y)$$

where E_p is the energy of the proton in MeV and Y is the neutron yield per mA of incident protons on the lithium target. When testing the advantage of different assembly designs at variable proton energies, for a given constant RUFTED, one would ideally prefer the highest possible useful flux per accelerator power. Or, for a given constant $\Phi_{u/P}$, one would prefer the highest possible RUFTED.

Each assembly was modeled using MCNP and the parameters RUFTED and $\Phi_{u/P}$ were calculated from the neutron flux energy spectrum at the irradiation point, 3 cm from the front of the beam port. The dose components of RUFTED were calculated by folding neutron and gamma fluxes with ICRU-46 adult (M) average

soft tissue kerma factors¹⁴ at the irradiation point. As previously described, the entire angle and energy dependent neutron distribution from the Lithium target is used in the MCNP model of the neutron source. This was done for different incident proton energies between 2.1 MeV and 2.6 MeV. For each energy on each assembly design, different moderator thicknesses were modelled to determine the RUFTED and $\Phi_{u/P}$ at each proton beam energy as a function of moderator thickness. Finally, graphs of RUFTED and $\Phi_{u/P}$ vs. moderator thickness were plotted for each proton beam energy. Two of these graphs are shown in Fig. 6.

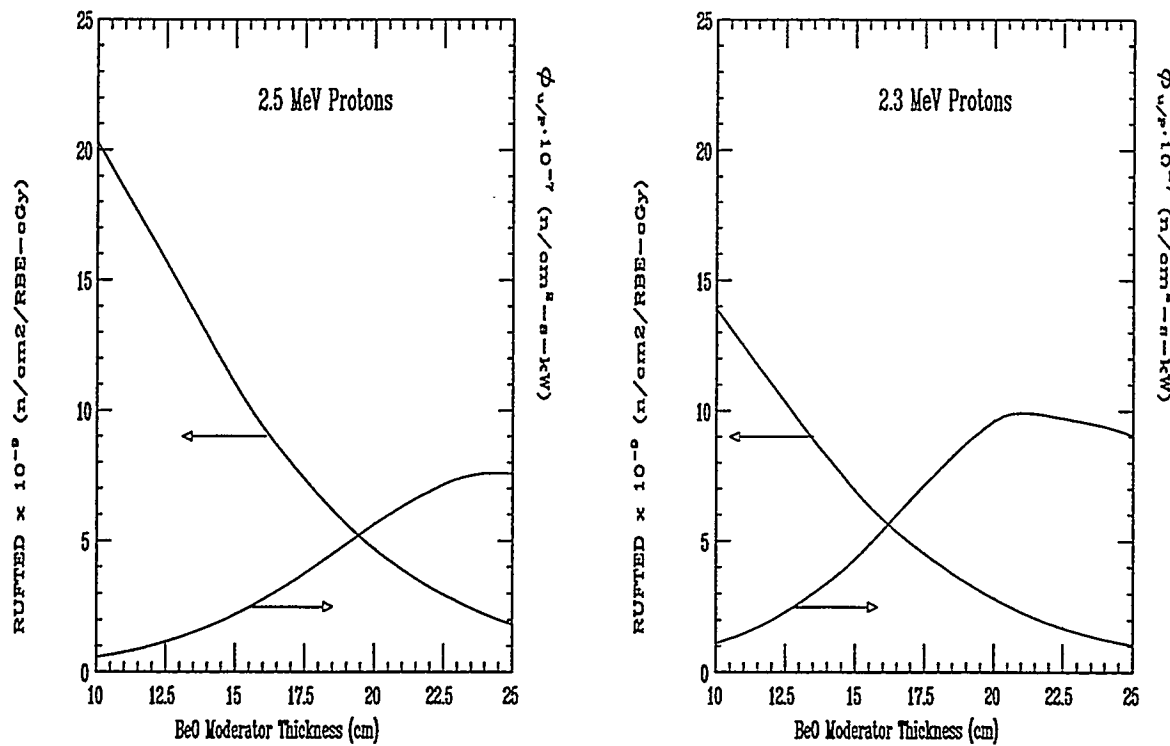


Figure 6: RUFTED & $\Phi_{u/P}$ vs. moderator thickness, BeO moderator (Assembly design #1). 2.5 MeV incident protons are shown on the left and 2.3 MeV protons on the right.

From these graphs, the exact moderator thickness necessary for a particular parameter value (RUFTED or $\Phi_{u/P}$) can be determined, as well as the value of the other parameter. A constant value of each parameter can then be taken to determine the effect of proton beam energy on the other parameter.

Each assembly design has already been optimized by the authors for protons at 2.5 MeV. For instance, Blue² has determined that 20.0 cm is the optimum BeO moderator thickness for design #1 at 2.5 MeV, taking into account the relative tradeoffs between RUFTED gain and $\Phi_{u/P}$ loss with increasing thickness. The RUFTED and $\Phi_{u/P}$ at this thickness can be read from the left plot of Fig. 6 and are found to be 5.63×10^9 n/(cm² RBE-cGy) and 4.69×10^7 n/(cm²-s-kW), respectively. If each of these parameters is left constant, the value of the corresponding parameter at 2.3 MeV can be determined from the appropriate moderator thickness in the right side of Fig. 6. An approximately constant RUFTED of 5.64×10^9 n/(cm² RBE-cGy) is achieved with only a 16.3 cm BeO moderator at 2.3 MeV, resulting in a higher $\Phi_{u/P}$ of 5.59×10^7 n/(cm²-s-kW). Similarly, to achieve a constant nearly $\Phi_{u/P}$ of 4.74×10^7 n/(cm²-s-kW) at 2.3 MeV, a 17.2 cm BeO moderator is needed, resulting in a higher RUFTED of 6.81×10^9 n/(cm² RBE-cGy).

Such an improvement in beam quality can be seen by comparing the energy spectra of each neutron beam at the irradiation point for these two different configurations. The increase in the number of useful neutrons for a given RUFTED and accelerator power is shown in Fig. 7[†], which contains two histograms of neutron spectra as a function of energy for equal RUFTEDs with 2.5 MeV and 2.3 MeV incident protons. Again, this figure applies to assembly design #1, which contains a BeO moderator. An incident proton energy of 2.5 MeV gives a RUFTED of 5.63×10^9 n/(cm² RBE-cGy) and a $\Phi_{u/P}$ of 4.69×10^7 n/(cm²-s-kW) (or 1.17×10^9 n/(cm²-s) for 10 mA). An incident proton energy of 2.3 MeV gives a RUFTED of 5.64×10^9 n/(cm² RBE-cGy) and a $\Phi_{u/P}$ of 5.59×10^7 n/(cm²-s-kW).

When $\Phi_{u/P}$ is taken as constant, the effect of a higher RUFTED is a lower unwanted patient dose. The energy-dependent contributions to dose from both neutrons and photons (created by neutron reactions in the assembly) for a constant $\Phi_{u/P}$ is shown in Fig. 8.

[†] All semi-log plots in this paper use 5 equal logarithmic intervals per decade to preserve spectral shape. Flux values on these plots have not been divided by this interval (0.2) and therefore should not be multiplied by this interval when integrating.

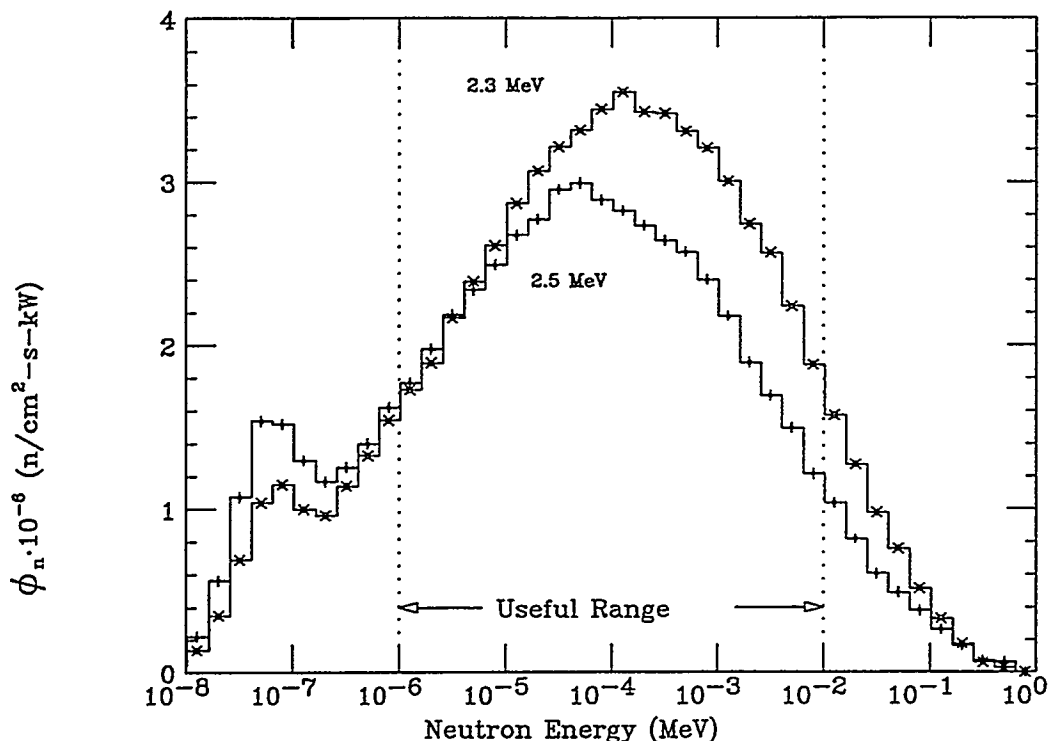


Figure 7: Neutron flux, Φ_n vs. energy for 2.3 MeV protons with 16.3 cm BeO moderator and 2.5 MeV protons on 20.0 cm BeO moderator. These two spectra have an identical RUFTED.

Note that lower energy protons also result in a lower photon dose to the patient, since fewer neutrons are initially necessary in the smaller moderator to create the same useful flux at the irradiation point. Thus, the fewer neutrons transporting through the assembly result in fewer (n,γ) reactions. Additionally, even though many of the higher energy neutrons are moderated to lower energies in the beam shaping assembly the primary contribution to the total dose to the BNCT patient is due to these fast neutrons. The primary advantage of a lower energy proton beam is the decreased production of these fast neutrons which contribute most of the dose to patient.

This analysis of a particular assembly can be expanded to include many different proton energies. By graphing the values of a single parameter (RUFTED or $\Phi_{u/P}$) while the other is left constant for a range of proton energies, the optimum proton

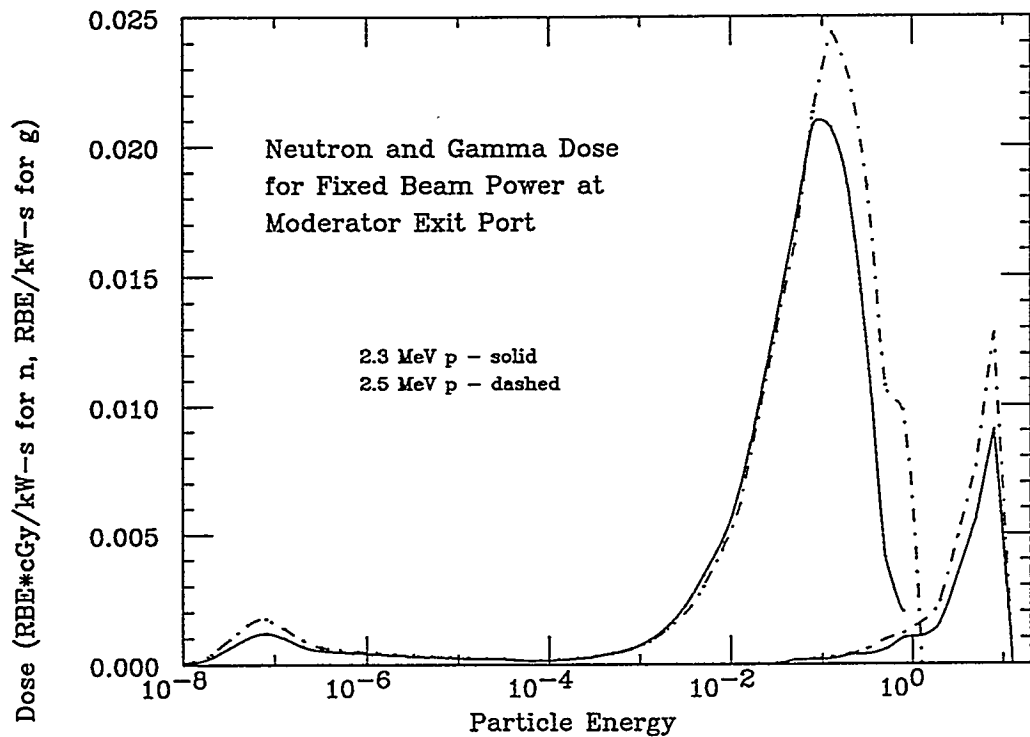


Figure 8: Neutron and gamma dose from BeO moderator design assembly #1 as a function of energy for 2.3 MeV incident protons (solid) and 2.5 MeV protons (dashes). The thermal and epithermal peaks represent neutron dose while the high energy peak represents the gamma dose. These spectra (17.2 cm BeO for 2.3 MeV protons, 20.0 cm BeO for 2.5 MeV protons) produce an identical Φ_u/P .

energy can be determined. The values of each of these parameters as a function of incident proton energy for assembly design #1 is shown in Fig. 9.

The optimum accelerator energy is the value at which these parameters are at a maximum. While the two maxima do not exactly coincide, they do not differ much, indicating that the optimum proton energy for an assembly such as this is in the range of 2.3 MeV to 2.35 MeV, not 2.5 MeV, which has previously been popularly assumed to be the optimum operating accelerator energy. Additionally, an even lower energy of 2.2 MeV results in parameters similar to those at 2.5 MeV. This indicates that a BNCT design that ordinarily requires a 2.5 MeV accelerator can use a 2.2 MeV accelerator with little change in beam quality, or a 2.3 MeV accelerator with better beam quality.

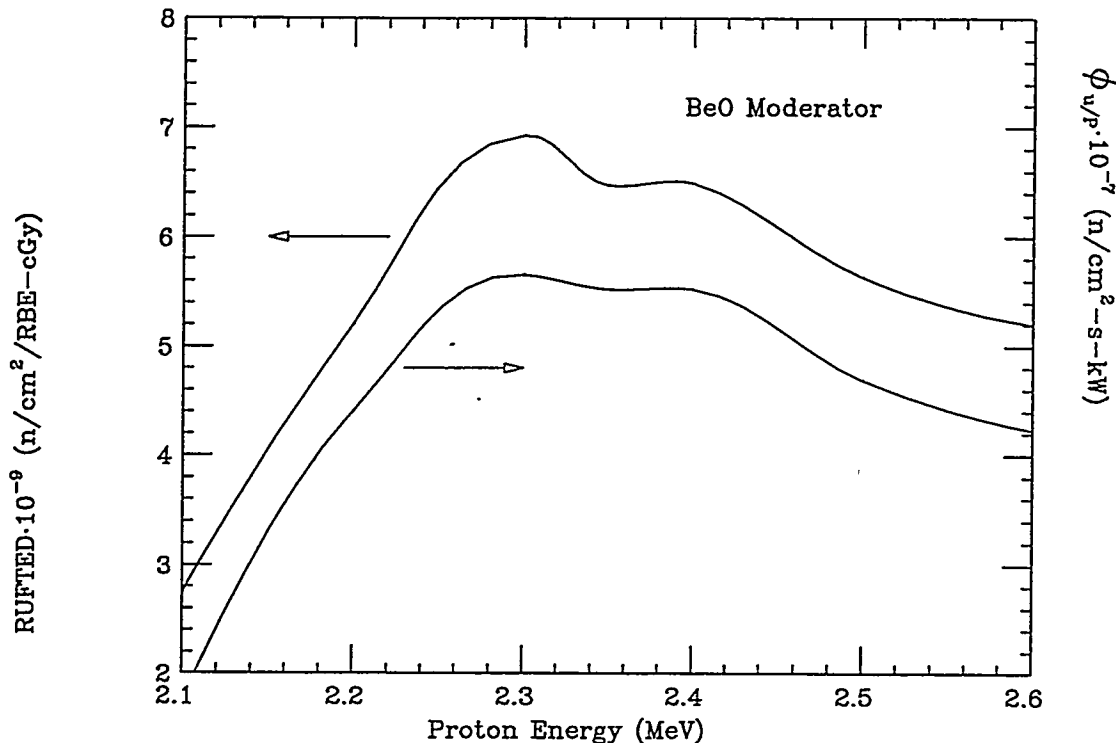


Figure 9: RUFTED & $\Phi_{u/P}$ vs. proton energy and BeO moderator (Assembly design #1) for various proton energies. For RUFTED values the $\Phi_{u/P}$ was held constant at 4.69×10^7 ($n/cm^2\text{-s-kW}$). For $\Phi_{u/P}$ values the RUFTED was held constant at 5.63×10^9 ($n/cm^2/\text{RBE-cGy}$).

Similar results are found when the same procedure is used to determine the optimum proton energy for other assembly designs. Fig. 10, Fig. 11 and Fig. 12 show the RUFTED and $\Phi_{u/P}$ as a function of proton energy for assemblies #2–#4, respectively.

These results are useful primarily as a rough estimate of the optimum proton energy for each assembly design. Both assembly designs #1 and #2 appear to function best at accelerator energies of near 2.3 MeV, with a sharp drop in beam effectiveness below this energy.

Assembly design #3, which consists primarily of a ^7LiF moderator with 1 cm of lead at the end of the assembly near the irradiation point, does not show the same peak in beam effectiveness at 2.3 MeV. Instead, a peak occurs at 2.6 MeV. Additionally, this design can be used with lower beam energies down to 2.3 MeV

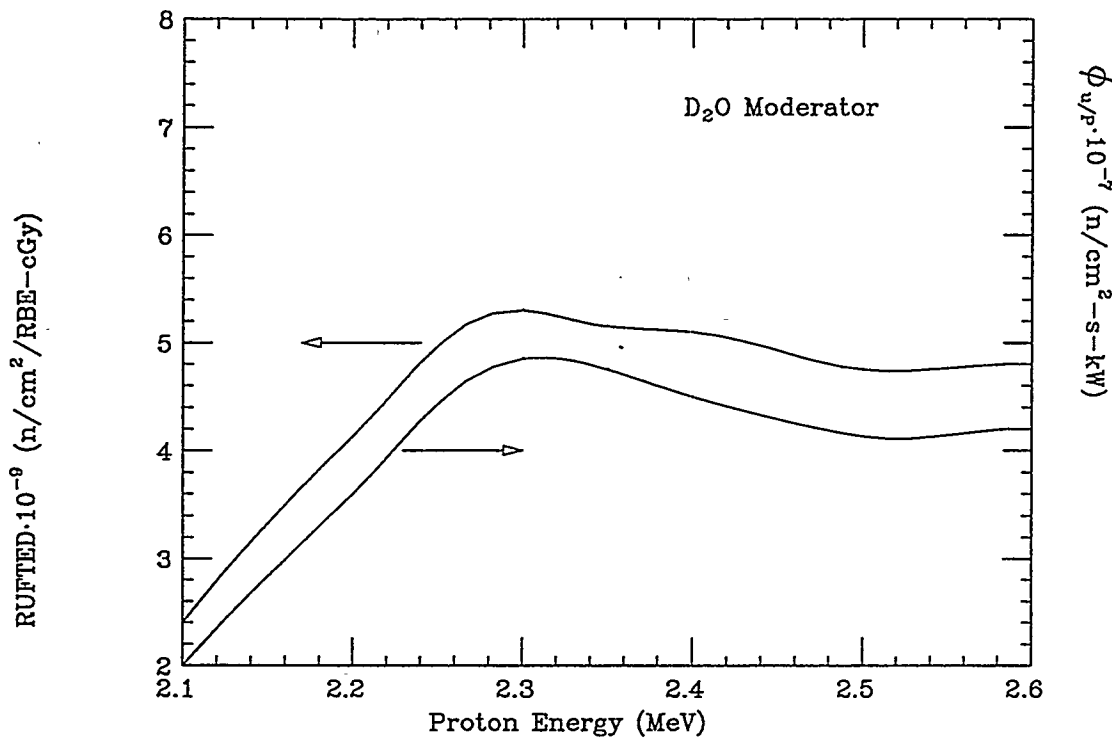


Figure 10: RUFTED & $\Phi_{u/P}$ vs. moderator thickness, D₂O moderator (Assembly design #2). For RUFTED values the $\Phi_{u/P}$ was held constant at 4.13×10^7 (n/cm²-s-kW). For $\Phi_{u/P}$ values the RUFTED was held constant at 4.75×10^9 (n/cm²/RBE-cGy).

- 2.35 MeV before significant losses in beam effectiveness occur. There are several difficulties involved in the analysis of this particular assembly design, however. First, assembly #3 contains two material zones. In simulations, only the thickness of the ⁷LiF was varied. The thickness of lead was left constant at 1 cm. Therefore, the exact configurations may not have been properly optimized for each proton energy, with error becoming more pronounced at lower proton energies, where much smaller moderator thicknesses are required.

A second more general concern is that the method of optimizing a BNCT neutron beam with a parameter such as the RUFTED is not ideal. A proper treatment would involve modeling the transport of the resultant neutron beam through a BNCT-treated phantom head. Unfortunately, additional factors become prevalent, such as the tumor depth, the boron loading in tumor, the boron loading in healthy

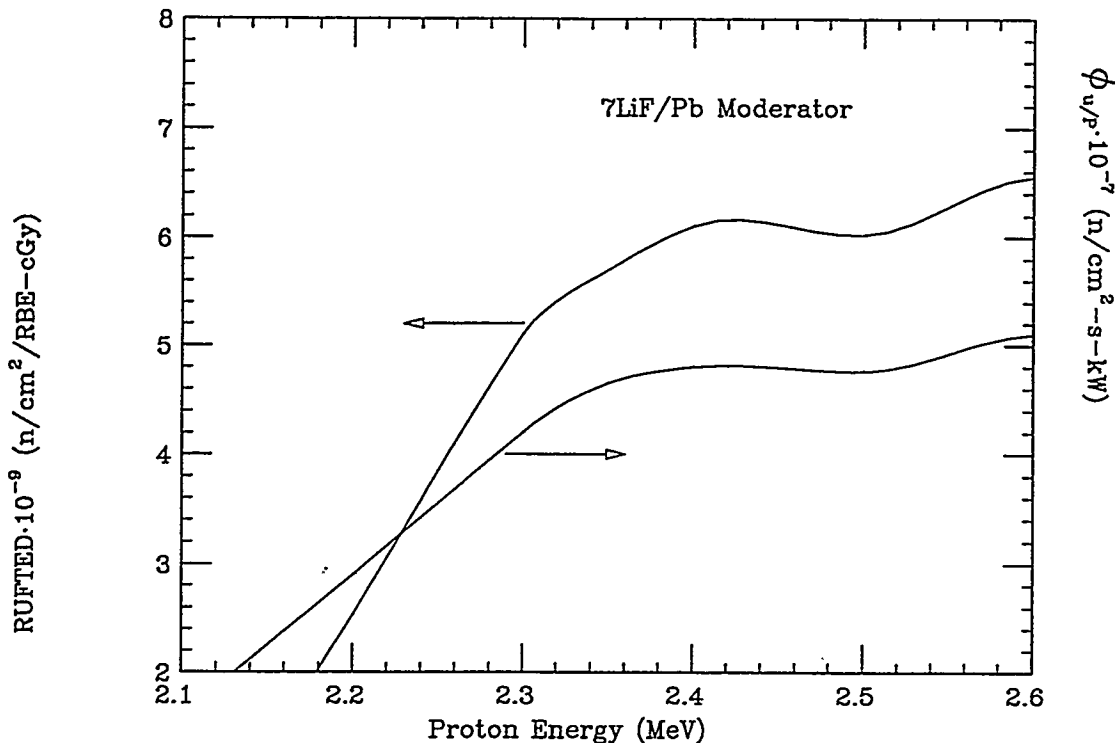


Figure 11: RUFTED & $\Phi_{u/P}$ vs. moderator thickness, $^7\text{Li}/\text{Pb}$ moderator (Assembly design #3). For RUFTED values the $\Phi_{u/P}$ was held constant at 4.76×10^7 ($n/cm^2\text{-s-kW}$). For $\Phi_{u/P}$ values the RUFTED was held constant at 6.02×10^9 ($n/cm^2/\text{RBE-cGy}$).

tissue, and the tumor size and shape. A simple analysis of the value of a particular neutron beam would become tedious. Such an analysis is, however, eventually necessary, as the RUFTED does not always take into account major differences in the particular shapes of neutron beams produced by a specific moderator. Figure 13 shows the different neutron spectra of two beams produced by two different assembly designs (#1 and #3) which have nearly equal $\Phi_{u/P}$'s and both spectrums are produced by 2.5 MeV incident protons. The spectrum produced by assembly #3 is more energetic with a higher percentage of fast neutrons within the useful flux range of 100 eV - 10 keV as is shown in Fig. 13.

Finally, assembly design #4, which is similar in construction to assembly design #2 with differences in the reflecting medium, shows a similar behavior with

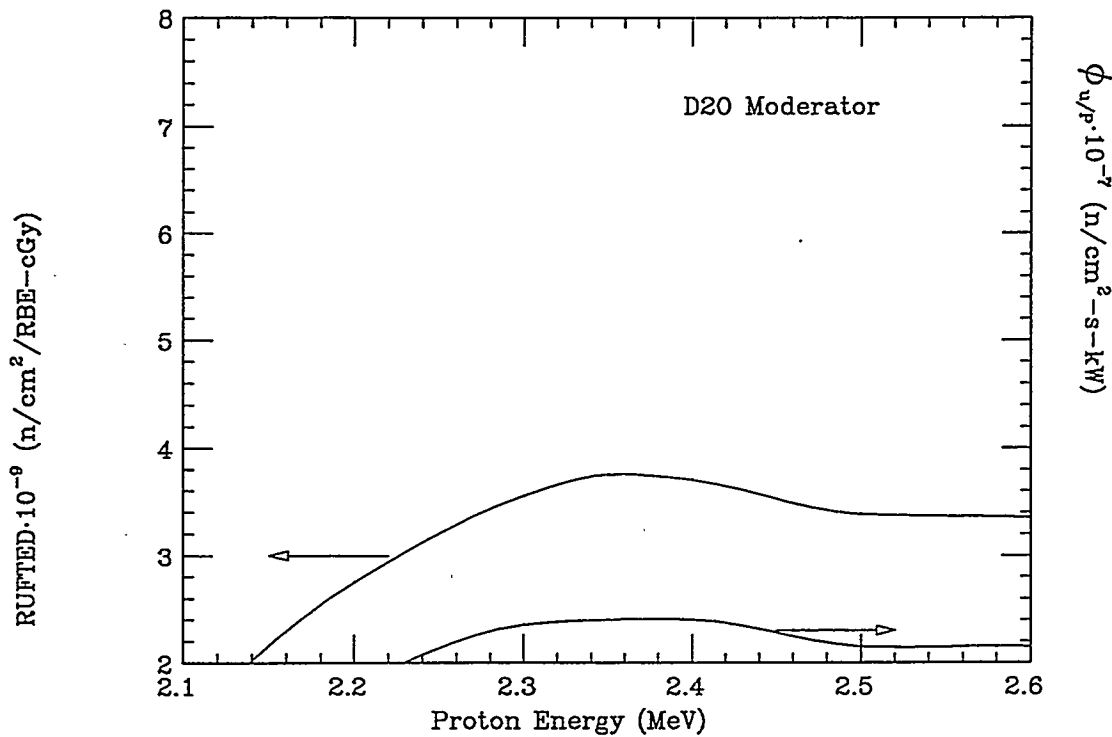


Figure 12: RUFTED & $\Phi_{u/P}$ vs. moderator thickness, D₂O moderator (Assembly design #4). For RUFTED values the $\Phi_{u/P}$ was held constant at 2.15×10^7 (n/cm²-s-kW). For $\Phi_{u/P}$ values the RUFTED was held constant at 3.35×10^9 (n/cm²/RBE-cGy).

changing proton energy as assemblies #1 and #2. The main differences are a less pronounced effect and a slightly shifted and broadened peak, centered instead at around 2.35 MeV. It is possible that 2.5 MeV is not necessarily the optimum energy at which to operate a proton accelerator for BNCT applications.

The optimal designs for each assembly have been listed in Table 3, along with the percent improvement that can be realized in either RUFTED or $\Phi_{u/P}$, compared to performance at 2.5 MeV.

This paper has demonstrated the possibility that one may achieve either higher or comparable useful neutron fluxes and beam qualities at energies lower than the often accepted value of 2.5 MeV. This is based on an optimization of parameters

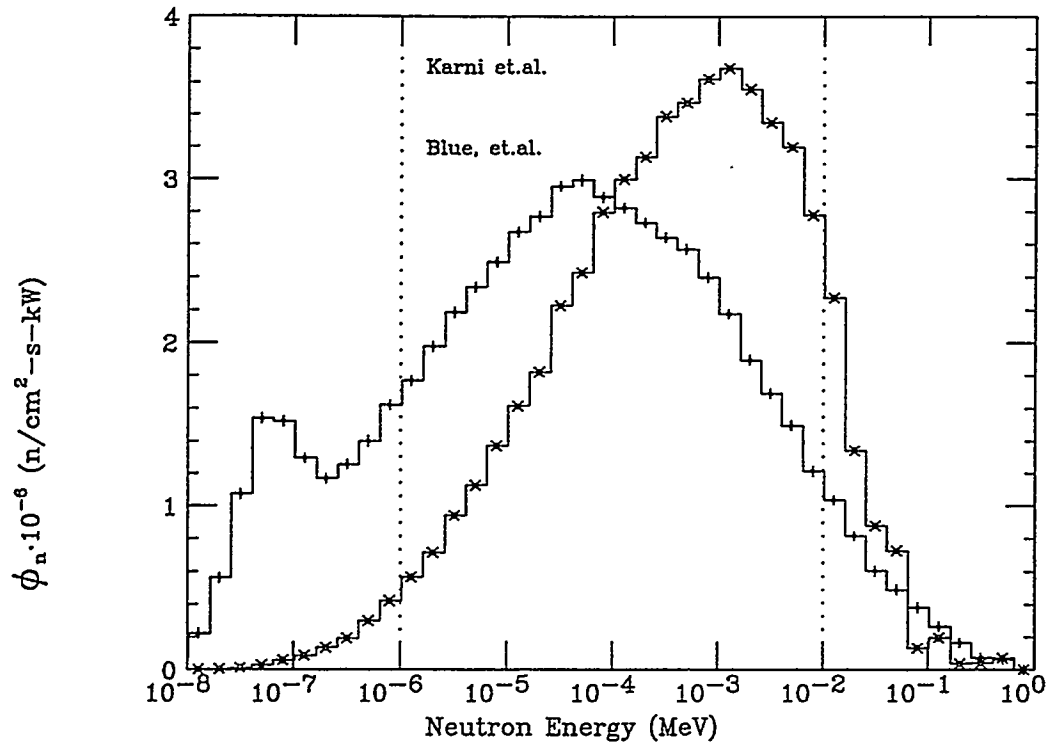


Figure 13: Neutron spectral shape for assembly designs #1 (BeO moderator by Blue) and #3 ($^7\text{Li}/\text{Pb}$ by Karni). The $\Phi_{u/P}$ in both cases is about equal to 4.7×10^7 (n/cm 2 -s-kW). Both spectrums are produced from incident 2.5 MeV proton beams.

in air at the patient irradiation point and not on an optimization of the depth-dose profile in tissue/tumor. To verify this, better figures of merit than the $\Phi_{u/P}$ and RUFTED should be found that can be used to compare spectra outside the moderator port without having to perform detailed patient treatment planning for each design parameter change and patient/tumor configuration.

Table 3: Design assembly analysis summary. The reference design, referred to in the last column, is the 2.5 MeV proton energy design specified in the first row of each assembly design #.

	Assembly Design	RUFTED (n/cm ² -RBE-cGy)	Φ_u/P (n/cm ² -s-kW)	% Increase in Given Quantity Over Reference Design
#1	2.5 MeV 20.0 cm BeO	5.63×10^9	4.69×10^7	(Reference #1)
#1	2.3 MeV 16.3 cm BeO	5.64×10^9	5.59×10^7	19.2% Φ_u/P
#1	2.3 MeV 17.2 cm BeO	6.81×10^9	4.74×10^7	21.2% RUFTED
#2	2.5 MeV 25.0 cm D ₂ O	4.75×10^9	4.13×10^7	(Reference #2)
#2	2.3 MeV 20.8 cm D ₂ O	4.69×10^9	4.72×10^7	14.4% Φ_u/P
#2	2.3 MeV 21.8 cm D ₂ O	5.30×10^9	4.10×10^7	11.6% RUFTED
#3	2.5 MeV 30.0 cm 7LiF	6.02×10^9	4.76×10^7	(Reference #3)
#3	2.6 MeV 31.8 cm 7LiF	6.00×10^9	5.10×10^7	7.1% Φ_u/P
#3	2.6 MeV 32.6 cm 7LiF	6.55×10^9	4.75×10^7	8.8% RUFTED
#4	2.5 MeV 25.0 cm D ₂ O	3.38×10^9	2.15×10^7	(Reference #4)
#4	2.35 MeV 22.3 cm D ₂ O	3.35×10^9	2.39×10^7	11.1% Φ_u/P
#4	2.35 MeV 23.0 cm D ₂ O	3.70×10^9	2.14×10^7	9.5% RUFTED

Acknowledgements

One of the authors (RJD) wishes to thank Martin Gelbaum for help in overcoming developmental deficiencies in fortran debugging and Peter Seidl for help with coordinate system transformations.

References

1. J. S. Hill *et al.*, "Selective Tumor Uptake of a Boronated Porphyrin in an Animal Model of Cerebral Glioma", Proceedings of the National Academy of Sciences of the United States of America, 89(5), 1785-1789 (1992).
2. J. W. Blue *et al.*, "A Study of Low Energy Proton Accelerators for Neutron Capture Therapy", proc. 2nd Int. Symp. Neutron Capture Therapy, October 18-21, 1985, pg. 147, H. Hatanaka, Ed., Nishimura Co., Ltd. (1985).
3. C. K. Wang, T. E. Blue and R. Gahbauer, "A Neutronic Study of an Accelerator Based Neutron Irradiation Facility for Boron Neutron Capture Therapy", Nuclear Technology Volume 84, 93-107 (1989).
4. N. Gupta "Fabrication and Preliminary Testing of a Moderator Assembly for an Accelerator-Based Neutron Source for Boron Neutron Capture Therapy", PhD Thesis, Ohio State University (1995).
5. H. Liskien and A. Paulsen, "Neutron production Cross Sections and Energies for the Reactions $^7\text{Li}(\text{p},\text{n})^7\text{Be}$ and $^7\text{Li}(\text{p},\text{n})^7\text{Be}^*$ ", Atomic Data and Nuclear Data Tables, 15, 57-84 (1975).
6. Herbert Goldstein Classical Mechanics, Addison Wesley Publishing Company (1980).
7. K. H. Beckurts and K. Wirtz, Neutron Physics, Springer-Verlag (1964).
8. J. F. Janni, "Proton Range-Energy Tables, 1 keV - 10 GeV", Atomic Data and nuclear Data Tables, Volume 27, Numbers 4/5, July/September (1982).

9. Y. Karni *et al.*, "Optimal Beam-Shaping Assemblies for BNCT Facilities using 2.5 MeV Protons on ^7Li or 19 MeV Protons on Be", Transactions of the American Nuclear Society Meeting, November (1995), San Francisco.
10. "MCNP-A A General Monte Carlo N-Particle Transport Code, Version 4A," LA-12625, J. F. Briesmeister, Ed. , Los Alamos National Lab. (1993).
11. J. C. Yanch, X-L. Zhou and G. L. Brownell, "A Monte Carlo Investigation of the Dosimetric Properties of Monoenergetic Neutron Beams for Neutron Capture Therapy", *Radiation Research* **126**, 1-20 (1991).
12. T. E. Blue, J. E. Wollard and N. Gupta, "Neutron RBE as a Function of Energy", Proceedings of the 8th International Conference on Radiation Shielding, April 24-28 (1994) Arlington, Texas, published by the American Nuclear Society.
13. E. L. Alpen and K. A. Frankel, "Biological Effectiveness of Recoil Protons from Neutrons of Energy 5 keV to 5 MeV", *Advances in Neutron Capture Therapy*, Edited by A. H. Soloway *et al.*, Plenum Press, New York (1993).
14. "Photon, Electron, Proton and Neutron Interaction Data for Body Tissues". ICRU Report 46, February 28 (1992).